SSRG International Journal of Geo-informatics and Geological Science
ISSN: 2393 – 9206 / https://doi.org/10.14445/23939206/IJGGS-V9I1P104

Volume 9 Issue 1, 28-37, Jan-Apr 2022

Original Article

Evaluation of Sea Surface Temperature based *p*CO_2 Algorithm in the Southwest Bay of Bengal

Ramalingam Shanthi[1], Durairaj Poornima[2], Ayyappan Saravanakumar[3], Rajdeep Roy[4], Saroj B. Choudhry[5]

[1,2,3]*Centre of Advanced Study in Marine Biology, Faculty of Marine Sciences, Annamalai University, Parangipettai, Tamilnadu, India.*
[4,5]*National Remote Sensing Centre, Balanagar, Hyderabad, Andhra Pradesh, India*

Received Date: 26 February 2022
Revised Date: 02 April 2022
Accepted Date: 15 April 2022

Abstract **-** *The partial pressure of carbon dioxide (pCO_2) is one of the most effective measurements of carbon dioxide in seawater, and the increases in pCO_2 profoundly affect the marine carbonate system. The role of SST on pCO_2 is analyzed to develop a regional pCO_2 algorithm using in-situ SST and calculated pCO_2 by employing the polynomial regression functions such as linear, quadratic, and cubic to develop a pCO_2 map and the best-fit algorithm of the cubic function developed for the postmonsoon season with an R^2 of 0.537 and SEE of ± 36.543 has been validated for remote sensing applications. Evaluation of satellite-derived pCO_2 with calculated pCO_2 showed R^2 of 0.498 and the root means square error (RMSE) of ±30.922 µatm with 75% of overestimation of calculated pCO_2 by the satellite-derived pCO_2. The satellite-derived pCO_2 map error is mainly because of the inbound errors in MODIS-derived SST products. Hence, improvement in sensor technology and retrieval algorithm would improve the retrieval of input parameters (SST), which is useful in estimating pCO_2 precisely. This would enable us to understand the biogeochemical processes behind the variability of CO_2 in the surface waters of the southwest Bay of Bengal.*

Keywords **-** *Chlorophyll, pCO_2, Regression, SST, Bay of Bengal, MODIS.*

I. INTRODUCTION

The global carbon cycle is essential for energy and mass exchange in the Earth System, as it connects the system's components (land, ocean, and atmosphere) (Garbe et al., 2014). Increases in atmospheric carbon dioxide (CO_2) concentrations, primarily caused by the combustion of fossil fuels, cement production, and increased urbanization, are directly accountable for 60% of the average global air temperature increase (IPCC, 2013). The direct exchange of CO_2 with the atmosphere at mixed-layer waters is primarily influenced by sea surface temperature (SST), dissolved inorganic carbon (DIC) levels, and total alkalinity (TA), with SST influenced by physical processes such as the mixing of water masses and DIC and TA influenced by biological processes (photosynthesis and respiration). The partial pressure of CO_2 (*p*CO_2) in seawater is generally modulated by both physical (SST) and biogeochemical (DIC and TA) processes (Lu et al., 2011).

The temperature mostly determines the pCO2 concentration at the sea surface at surface (SST). When seawater is warmed by 1°C, *p*CO_2 increases by four in a parcel with a fixed chemical composition (Stephans et al., 1995; Zhu et al., 2009). On the other hand, the DIC in the surface ocean varies from an average value of 2150 µmol kg^{-1} in Polar Regions to 1850 µmol kg^{-1} in the tropics as a result of biological processes and reduces *p*CO_2 by a factor of 4 (Feely et al., 2001). Therefore, the effect of biological drawdown and temperature on surface water *p*CO_2 is similar, but the two effects are often compensating. Hence, the spatial and temporal distribution of *p*CO_2 in surface waters and CO_2 flux is largely governed by a balance between the changes in seawater temperature, net biological utilization of CO_2, and the upwelling flux of CO_2-rich waters.

According to carbon dioxide measurements in the atmosphere, the oceans and terrestrial biosphere absorb roughly half of the annual anthropogenic CO_2 emissions (Siegenthaler and Sarmiento, 1993). Knowledge of the large-scale spatiotemporal variability in partial pressure of carbon dioxide (pCO_2) distribution is a prerequisite to estimating oceanic CO_2 absorption, which is difficult to obtain from observations only (Wallace, 1995). Several researchers have utilized various methods to interpolate and/or extrapolate shipboard pCO_2 data on spatial and temporal scales using relationships with remotely sensed data, such as sea surface temperature (SST) and chlorophyll-a concentration. For instance, Tans et al. (1990) and Keeling and Shertz (1992) used the relationship between pCO_2 and SST to infer surface ocean CO_2 fields. Stephens et al. (1995) with root-mean-square (RMSE) error of ($\leq$ 40 µatm). Ono et al. (2004) included chlorophyll *a*s an additional regression parameter and reduced the RMS error to $\leq$ 17µatm. Sarma et al. (2006) further developed a remote-sensing algorithm for pCO_2 by including SST, chlorophyll-a, and climatological salinity. Lohrenz and Cai (2006) added chromophoric dissolved organic matter (CDOM) to derive sea surface salinity as a parameter in their remote-sensing algorithm for pCO_2. Zhu et al. (2009) studied the air-sea exchange of CO_2 using remotely sensed pCO_2 developed using satellite-derived SST, chlorophyll *a*, and wind speed with an RMS error of 4.6 µatm. Recently, a regression equation for pCO_2 with SST and chlorophyll *a* was proposed by Zui et al. (2012) and Qin et al. (2014) with an RMSE of ±13.45 µatm and ±21.46 µatm with the satellite-derived pCO_2 respectively.

Considering the above facts, it is attempted to develop a regional pCO_2 algorithm using *in-situ* SST and calculated pCO_2. The best-fit algorithm has been validated with the calculated pCO_2 measurements for remote sensing applications.

II. MATERIALS AND METHODS

The present study was conducted along the Tamilnadu coast, falling along the southwest Bay of Bengal region. From January 2017 to June 2019, regular monthly samplings were performed at 1, 5, 7, 9, and 12 km from the coast at four sampling stations concealing the longitude and latitude of Chennai (80°23.9 E - 13°07.9 N), Cuddalore (79°48.5 E – 11°42.4 N), Parangipettai (79°51.7 E – 11°30.6 N) and Karaikal (79°55.5 E – 10°54.8 N) (Fig. 1). Based on the region's northeast monsoon, the study period was split into four seasons: postmonsoon (January to March), summer (April to June), premonsoon (southwest monsoon - July to September), and monsoon from October to December) (monsoon).

A. *In-situ* data

A digital multi-stem thermometer with a ± 0.1° C precision was employed to monitor in situ SST. Water samples were taken directly from the Niskin water sampler into a 250 ml polyethylene container.

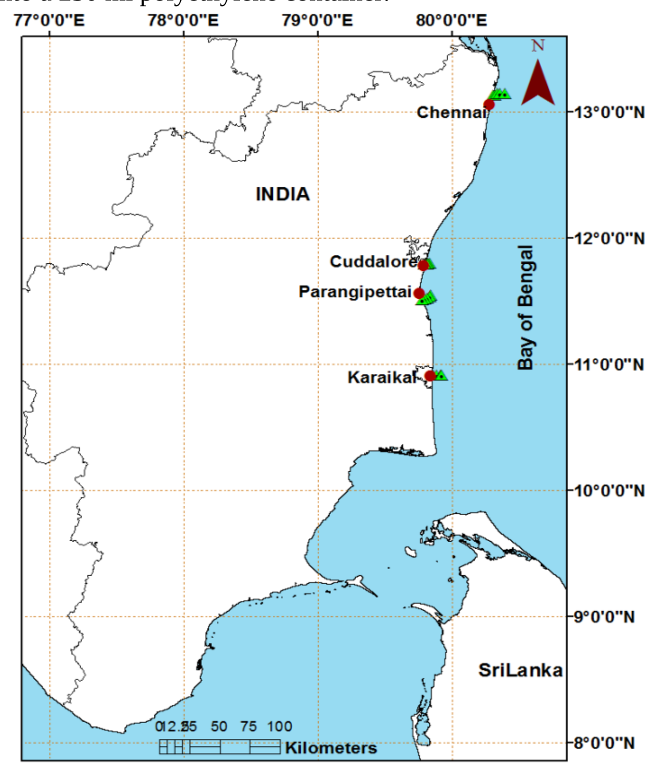

Fig. 1 Map showing the sampling stations and transects in the southwest Bay of Bengal water

clean drawing tubes with no bubbles and low turbulence with sufficient flushing to avoid contamination from the atmosphere. A hand-held refractometer was used to determine salinity (Atago hand refractometer, Japan). The samples were stored in the dark until further analysis of pH and total alkalinity (TAlk) that were measured in the laboratory using a potentiometric titrator calibrated on the total scale (905 Titrando, Metrohm, Switzerland) (Frankignoulle and Borges, 2001). The pCO_2 was computed using measured temperature, salinity, TAlk, and *in situ* pH (total scale). The precision for pCO_2 was 9–13 µatm (Bhavya et al., 2016).

B. SST based pCO_2 Retrieval Algorithm

SST is usually the key governing element of pCO_2 in oligotrophic waters, which provides a theoretical basis for calculating pCO_2 (Zhai et al., 2005). Hence, the *in situ* SST and calculated pCO_2 datasets were subjected to two-dimensional regressions to develop *the* pCO_2 algorithm. Three different polynomial functions such as linear, quadratic, and cubic were applied for regression analysis

C. Satellite Data

MODIS-Aqua derived Level-2a SST image was acquired to generate a remotely sensed pCO_2 image using satellite-derived SST. For remote sensing measurements in the southwest Bay of Bengal, February to May is a good time to get cloud-free data; however, only occasional data sets are available attributed to the influence of both the southwest and northeast monsoons, which render the southern Bay of Bengal a more cloud-prone region in the northern Indian Ocean during the rest of the year. As a result, MODIS-Aqua derived Level-2a SST for 23rd March 2014, with a spatial resolution of 1km, was obtained from http://modis.gsfc.nasa.gov. ERDAS IMAGINE (9.2. ver.) and ENVI (4.7. ver.) software-generated SST and pCO_2 images from the data. The geometric correction was used on the SST data to remove image distortion and bring it to a standard geographic projection (Lat/Lon) with a modified Everest Datum.

D. Evaluation Criteria

The evaluation was carried out by comparing satellite-derived values with field measurements. SigmaPlot (Ver.12.0) statistical software was used to perform statistical fitting on these data. Mean Normalized Bias (MNB) and Root Mean Square Error (RMSE) evaluated the algorithm's performance. Mean normalized bias measures whether true values are over or understated. Root mean square error is a reliable marker of data scatter for normally distributed variables and provides vital information on satellite and in-situ data (Shanthi et al., 2013).

III. RESULTS AND DISCUSSION

The oceanic partial pressure of CO_2 (pCO_2) is highly variable, and it is difficult to assess spatial and temporal variability because of the scarcity of measurements. In general, pCO_2 and SST have a strong relationship, mainly in oceanic regions where significant physical and biological factors are. The thermodynamic effect of temperature on pCO_2 (at constant salinity, alkalinity, and dissolved inorganic carbon) is about 4ºC (Copin-Montegut, 1989). At the same time, the equilibrium of the carbonate system in seawater is altered by the influence of SST in the absence of external exchanges (Qin et al., 2014). Hence, the two-dimensional approach of SST and pCO_2 regression fits are attempted to understand the role of SST on pCO_2 in the southwest Bay of Bengal coastal waters; the polynomial regression analysis for different functions like linear, quadratic, and cubic have been carried out to generate pCO_2 maps.

A. 2D-Regression Analysis and Pco₂ Algorithm Development

In-situ SST and calculated pCO_2 concentrations (Eq. 2) were obtained by monthly coastal samplings at four sampling stations from January 2017 to June 2019 in the southwest Bay of Bengal region. The data points (20) matching the date of satellite-derived SST data were treated separately for validation purposes. Finally, 334 points were taken for regression analysis accounting for 94% of the total data.

Where N= Number of points. On the whole cubic, the function was a better fit than other functions. It produced a significant relationship during the postmonsoon season (R^2=0.537) with a minimum standard error of estimation (± 36.543 µatm), and the derived pCO_2 algorithm was used to generate the pCO_2 images. The pCO_2 algorithm implies the following equation:

$$pCO_2 = 263581.4877 - 27820.7825*SST + 980.9763*SST^2 - 11.5396*SST^3$$

Postmonsoon

pCO_2=1590.7218–43.4352*SST $\rightarrow$ (1) Linear

pCO_2=-2922.0693+272.4418*SST–5.5244*SST^2 $\rightarrow$ (2) Quadratic

pCO_2=263581.4877–27820.7825*SST+980.9763*SST^2–11.5396*SST^3 $\rightarrow$ (3) Cubic

Summer

pCO_2 = 2594.7694–76.0582*SST $\rightarrow$ (4) Linear

pCO_2=9892.4125–555.7563*SST +7.8763*SST^2 $\rightarrow$ (5) Quadratic

pCO_2=-4167.8615+832.0346*SST–37.7442*SST^2–0.4995*SST^3 $\rightarrow$ (6) Cubic

Premonsoon

pCO_2 =2983.6552–88.1427*SST $\rightarrow$ (7) Linear

pCO_2=29285.3892–1881.4403*SST +30.5341*SST^2 (8) Quadratic

pCO_2=-151226.738+16636.935*SST–602.1762*SST^2–7.1998*SST^3 $\rightarrow$ (9) Cubic

Monsoon

pCO_2 = 2755.7601–77.9496*SST $\rightarrow$ (10) Linear

pCO_2=-2378.7502+283.9733*SST–6.3704*SST^2 (11) Quadratic

pCO_2=-596822.233-63293.5995*SST–2240.349*SST^2–26.443*SST^3 $\rightarrow$ (12) Cubic

B. Development of pCO₂ algorithm based on in-situ SST

The regression analysis of the full dataset for three polynomial functions reveals an insignificant association with an $R^2 \leq 0.330$ and SEE ≥ ±92µatm between SST and pCO_2. The thermal capacity of the ocean is very large, and it varies from season to season, and space coinciding with this pCO_2 also shows fluctuations. Hence it is not appropriate to treat the entire dataset in one cluster. Therefore, the seasonal regression analysis between SST and pCO_2 was made to develop an SST-based pCO_2 algorithm for three polynomial linear, quadratic, and cubic functions. The regression plots were illustrated in figures 2-5, and the polynomial regression equations were given as follows. SST plays a major role in influencing the seasonal variability of pCO_2 because temperature determines the solubility of CO_2 to a large extent (Sabine et al., 2000). Higher SST makes the air lighter, shifts the air to the upper atmosphere, and reduces the air-sea interaction, thereby CO_2 dissolution on the water's surface. In the regression analysis, SST portrays the constant negative relationship with pCO_2 in all the seasons, and it is clear from the regression equations that pCO_2 decreases with increasing temperature (Lefevre and Taylor, 2002). SST in the Bay of Bengal varies more seasonally, with high temperatures during the summer months and low temperatures during the monsoon and postmonsoon seasons, which coincide with river inputs and winter cooling. Hence it is attempted to treat them on a seasonal scale.

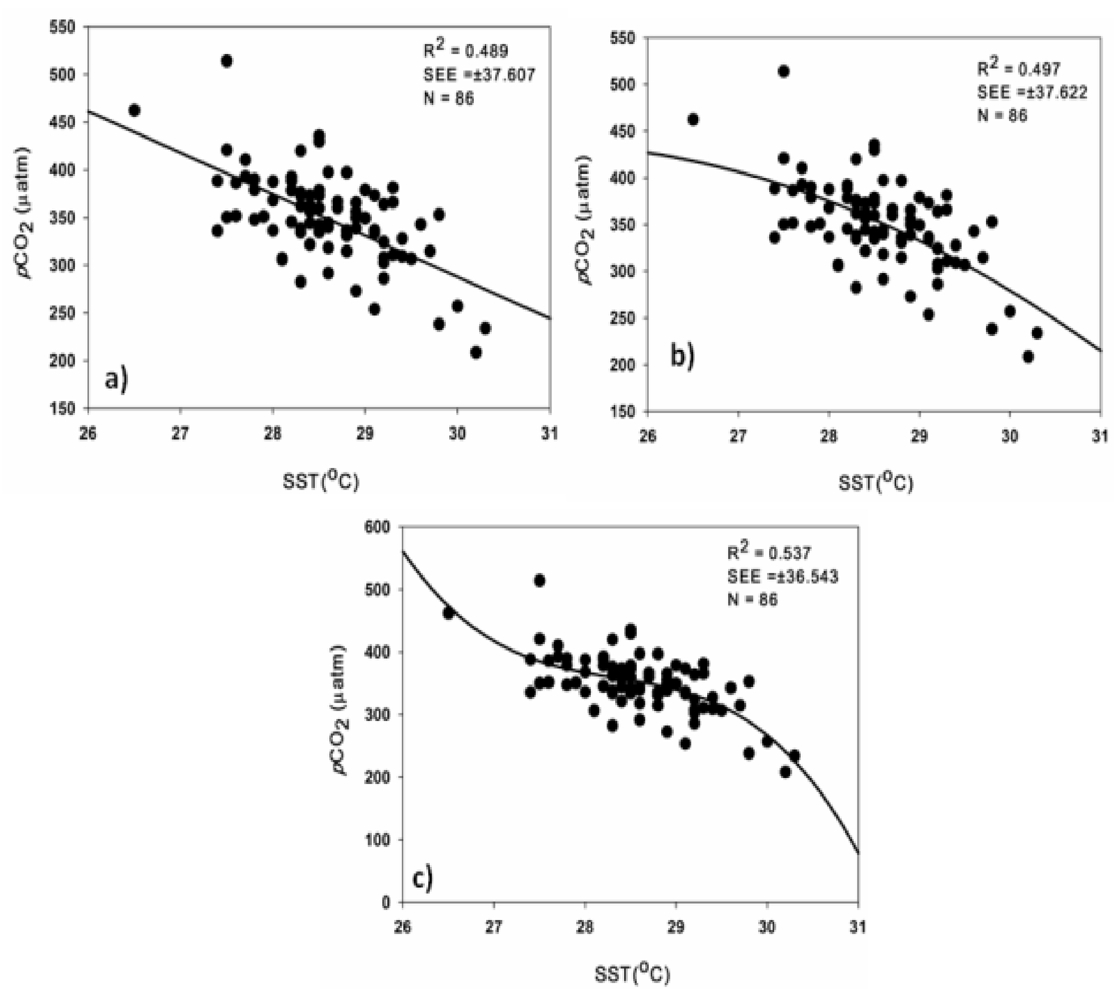

Fig. 2 Regression analysis of postmonsoon dataset between *in-situ* SST and calculated pCO_2 for linear (a), quadratic (b), and cubic (c) polynomial functions

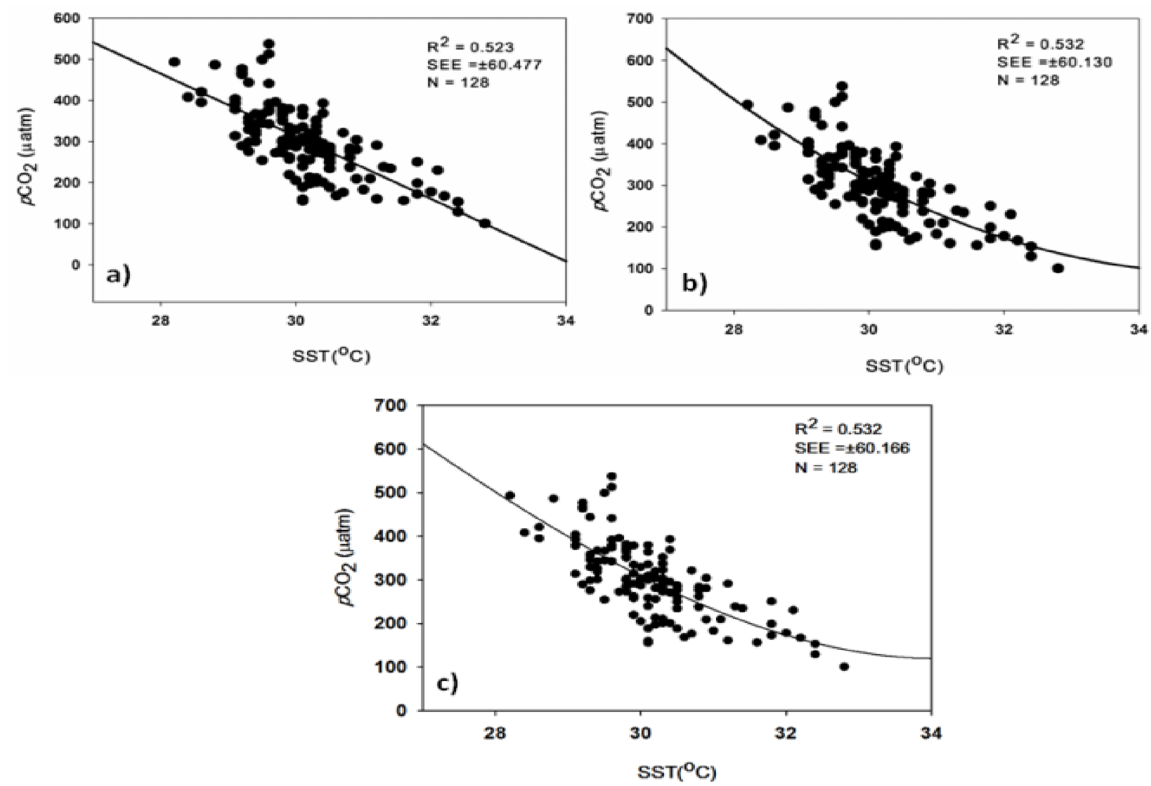

Fig. 3 Regression analysis of summer dataset between *in-situ* SST and calculated *p*CO_2 for linear (a), quadratic (b), and cubic (c) polynomial functions

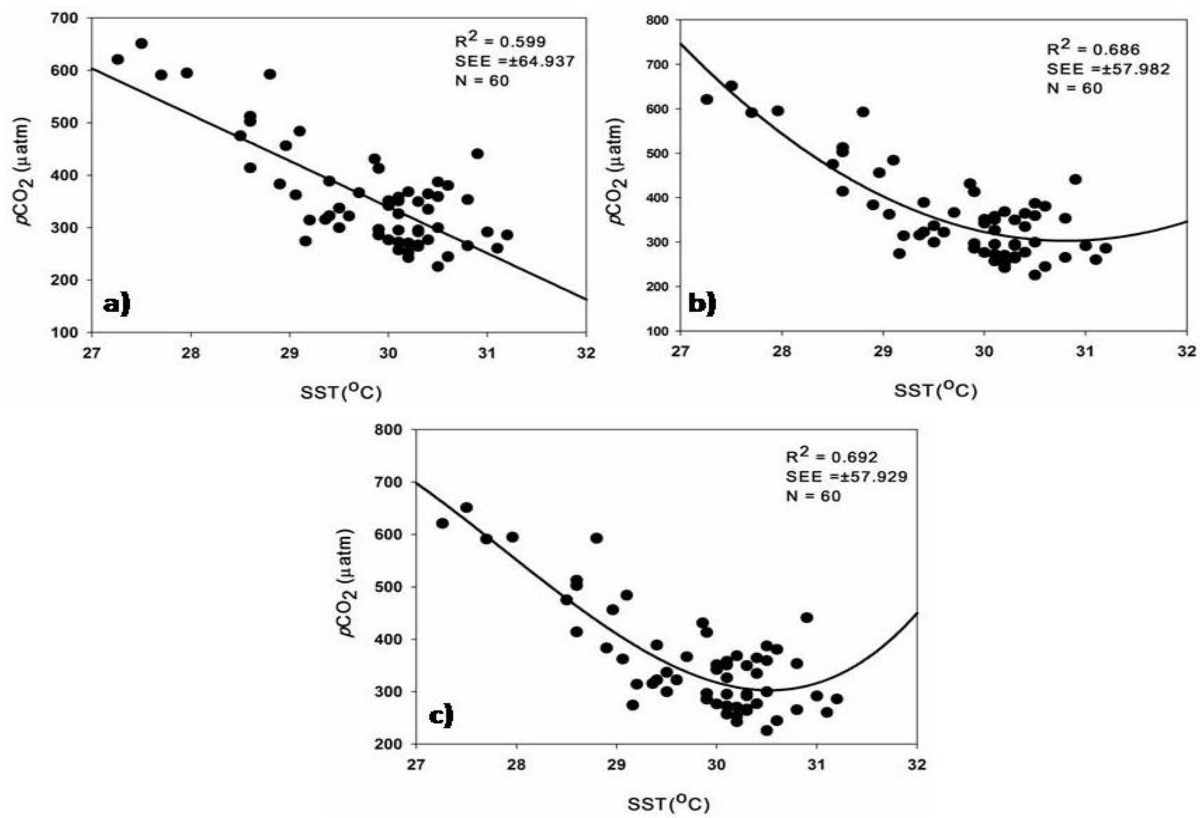

Fig. 4 Regression analysis of premonsoon dataset between *in-situ* SST and calculated *p*CO_2 for linear (a), quadratic (b), and cubic (c) polynomial functions

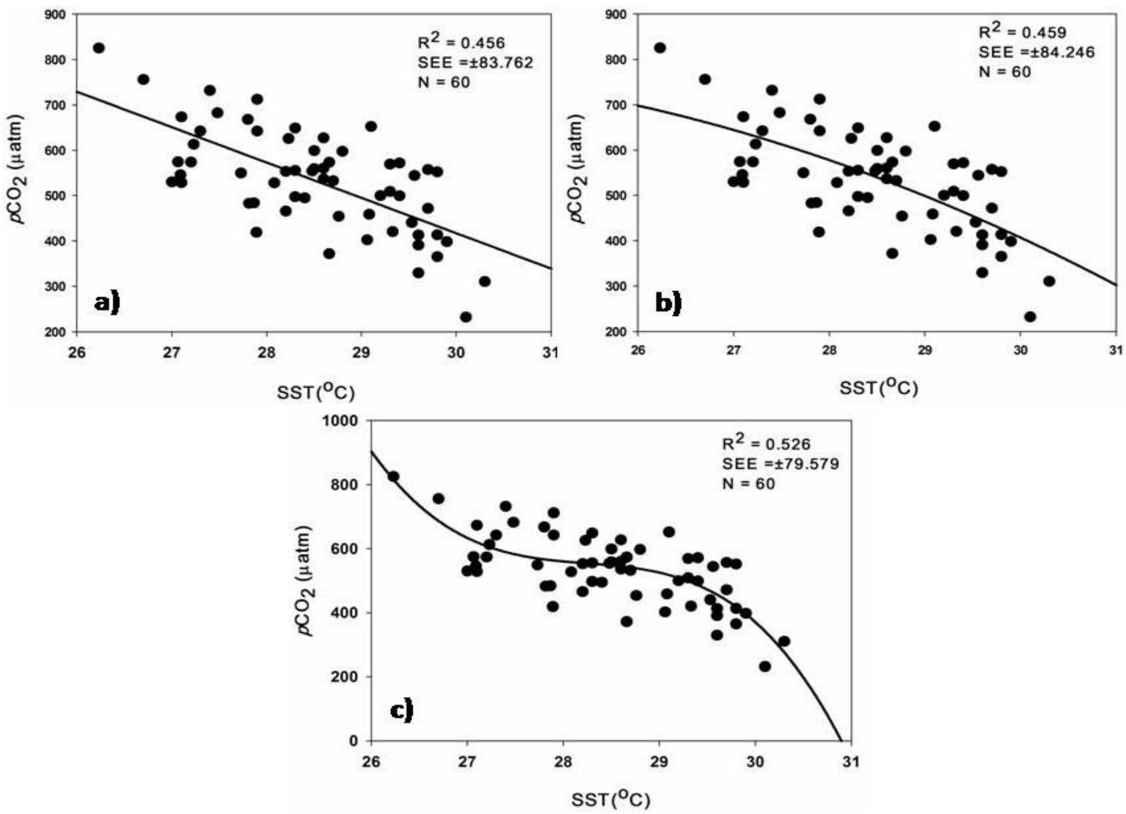

Fig. 5 Regression analysis of monsoon dataset between *in-situ* SST and calculated $p\mathrm{CO_2}$ for linear (a), quadratic (b), and cubic (c) polynomial functions

The R^2 values and standard error of estimate (SEE) obtained for different seasons using the polynomial regression analysis are summarized in table 1. Among the three polynomial functions used, the cubic function provided better agreement for all the seasons than other functions. Still, the standard error of the estimate remained high (> 50µatm) for summer, premonsoon, and monsoon seasons. The polynomial regression analysis of different seasons showed the significant R^2 values during pre-monsoon season (R^2 = 0.599, SEE = ±64.937; R^2 = 0.686, SEE = ±57.982 and R^2 = 0.692, SEE = ±57.929) for linear, quadratic, and cubic functions respectively than other seasons. So after that summer explained the better relationship between SST and $p\mathrm{CO_2}$ and poor correlation co-efficient is observed during monsoon and postmonsoon seasons with the R^2 values for different functions.

Table 1. Results of regression analysis between *in-situ* $p\mathrm{CO_2}$ and SST

Season		**Linear**		**Quadratic**		**Cubic**	
	N	**R^2**	**SEE(±)**	**R^2**	**SEE(±)**	**R^2**	**SEE(±)**
POM	86	0.49	37.61	0.50	37.62	**0.54**	**36.54**
SUM	128	0.52	60.48	0.53	60.13	0.53	60.17
PRM	60	0.60	64.94	0.69	57.98	0.69	57.93
MON	60	0.46	83.76	0.46	84.25	0.53	79.58

The cubic function provided a better predictive capability for all seasons with a marginal improvement in the correlation coefficient than the other two functions. Conversely, Olsen et al. (2008) investigated the different regression diagnostics from single parameter relationships of $f\mathrm{CO_2}$ with SST, chlorophyll *a*, and mixed layer depth. They found a poor correlation of SST with $f\mathrm{CO_2}$ in seawater during winter ($R^2 \leq 0.001$) and a strong correlation with chlorophyll *a* and mixed layer depth in summer. In the present study, the cubic function offers an improved correlation coefficient (R^2 = 0.537) during the postmonsoon season, with a minimum standard error of estimate (±36.543). Thus, a cubic function-derived algorithm has been applied to develop satellite-derived $p\mathrm{CO_2}$.

C. Evaluation of SST based pCO₂ algorithm

To generate a satellite-derived pCO_2 field, MODIS-Aqua retrieved SST data was used for the postmonsoon season (23rd March 2014) (Fig. 6). Satellite-derived SST (MODIS-Aqua) and modeled pCO_2 images are validated with the *in-situ* SST and calculated pCO_2 data of the same date at different locations of the southwest Bay of Bengal. Evaluation of MODIS-SST with *in-situ* SST shows a negative bias (MNB = -0.009) with RMSE of ±0.491ºC (Fig.7a), which is greater than the error (±0.38°C) observed by Gentemann (2014) and could be attributed to possible errors in cloud removal, contaminated aerosol retrievals, or sampling. Moreover, SST measured using infrared radiometers will estimate with high resolution only under cloud-free conditions, and it has been evident from the regression results (R^2=0.700 and SEE ±0.244ºC). The data points fall outside the 95% confidence band, suggesting that the satellite-derived values were higher or lower than they should be in natural waters. However, a comparison plot of in-situ SST with MODIS-derived SST revealed that the MODIS-SST, scattered about the 1:1 line, underestimated 70% of the in-situ data and inflated 30% of the in-situ data (Fig.7b).

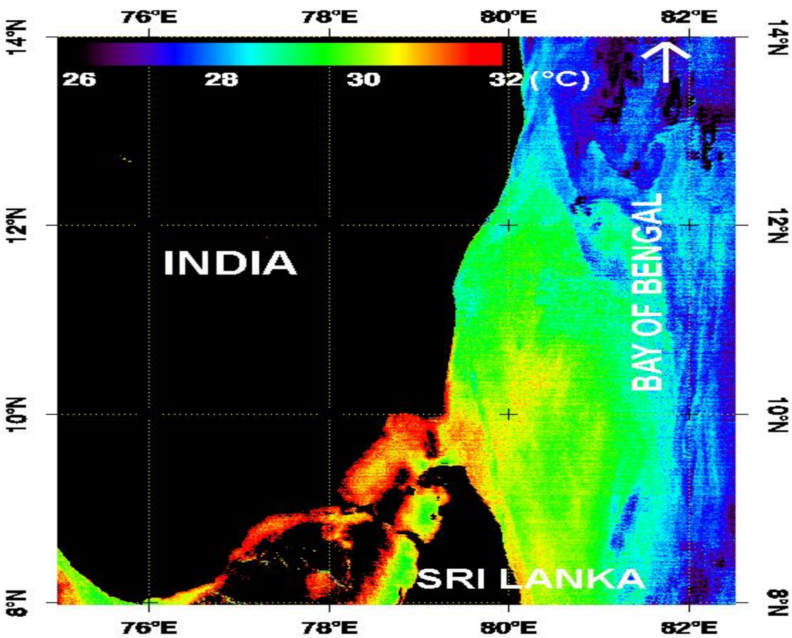

Fig. 6 MODIS-Aqua derived SST image of 23rd March 2014

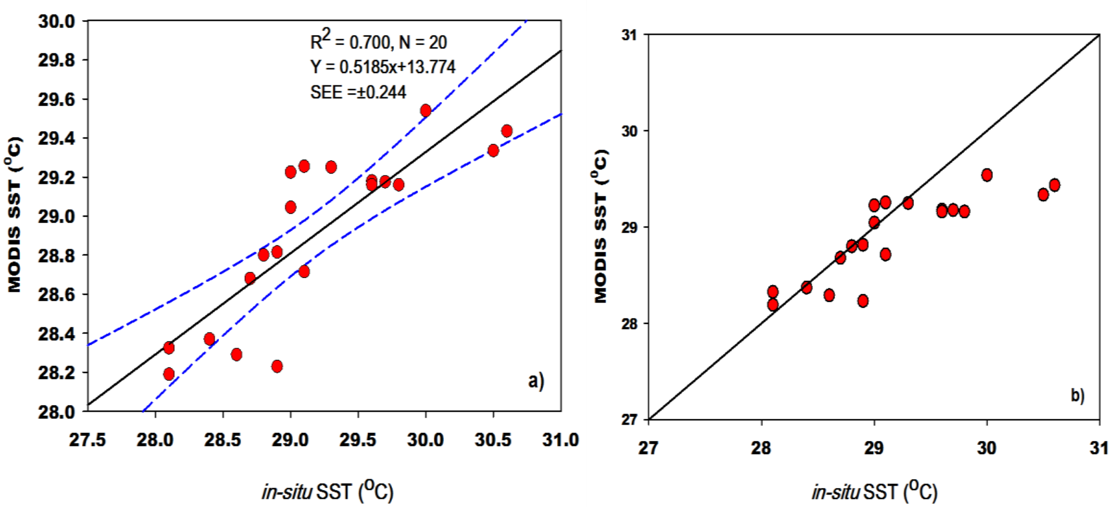

Fig. 7 Regression (a) and comparison (b) plots of *in-situ* SST Vs. MODIS-Aqua derived SST

The statistical results reported in this study are analogous to MODIS SST validation using *in-situ* observations along the western Pacific coasts (Barton and Pearce, 2006) with a bias of –0.32°C; western North Pacific (Hosoda et al., 2007) with a bias of –0.06°C and RMSE of ±0.81°C, Taiwan coast (Lee et al., 2010) with a bias of 0.42°C and RMSE of ±0.86°C, San Matías Gulf of Argentina (Williams et al., 2013) with an R^2 of 0.89 and Bay of Bengal (Narayanan et al., 2013) with a bias of

1.80°C and reported the overestimation of the satellite product. However, with a correlation of R^2 = 0.700, the regression fit was determined to be substantial. Hence MODIS-derived SST data was used to construct an SST-based pCO_2 algorithm to generate remotely sensed pCO_2.

D. Validation of Remotely Sensed pCO₂

The algorithm developed for the postmonsoon season is applied with MODIS-Aqua-derived SST to generate the remotely sensed pCO_2 fields. The algorithm's predictive capability has been examined by comparing the calculated pCO_2 with remotely remote sensed pCO_2 data. Validation of remotely sensed pCO_2 was carried out to assess the SST-based algorithm's performance by using calculated pCO_2 data (Fig.8). The validation results found that there is no significant coefficient of determination (R^2 = 0.428) with the SEE of ±12.510, MNB (0.071), and RMSE (30.922), indicating the poor agreement between remotely sensed pCO_2 and calculated pCO_2 (Fig.9a). A comparison plot of remotely sensed pCO_2 with calculated pCO_2 showed 75% overestimation and 25% underestimation of calculated pCO_2 data (Fig. 9b). Similarly, Metzl et al. (1995) observed seasonal pCO_2–SST relationships to reconstruct pCO_2 from climatological SST in the Indian and Antarctic Oceans. Stephans et al. (1995) also used the pCO_2-SST relationship to extrapolate pCO_2 distribution by using satellite-derived SST in the North Pacific basin and obtained an RMSE of ±17 µatm and ±40 µatm for the northeast and western Pacific. The change is due to the impact of biologically produced variations in DIC.

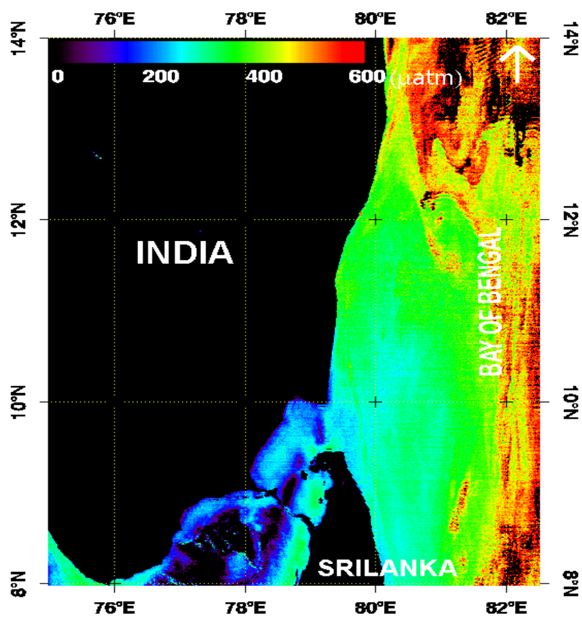

Fig. 8 SST based satellite-derived pCO_2 image for 23rd March 2014

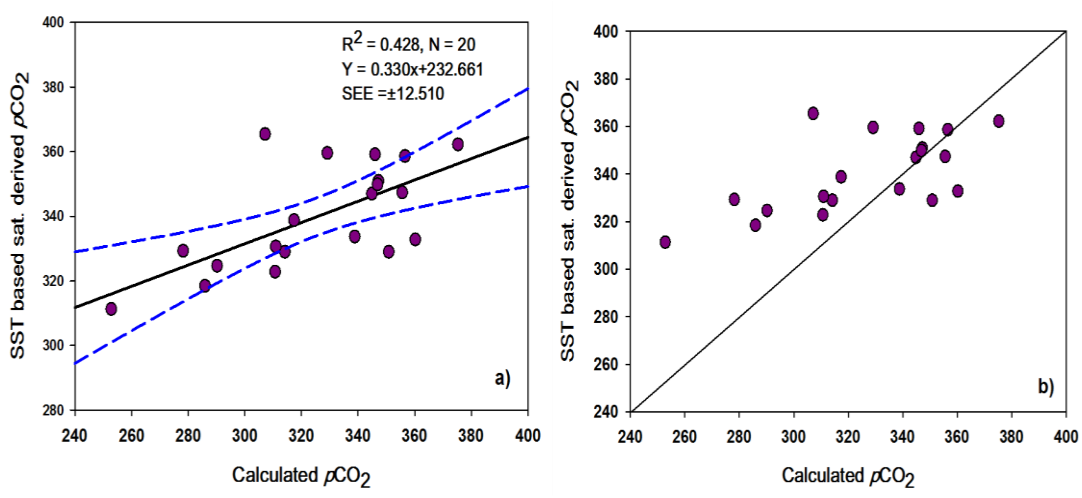

Fig. 9. Regression (a) and comparison (b) plots of calculated pCO_2 Vs. SST-based satellite-derived pCO_2.

Landrum et al. (1996) and Lee et al. (1998) described the relation of pCO_2 with SST in subtrophic and subarctic (30-43ºN) waters and found an insignificant correlation (R^2 = 0.38). These results indicated that SST alone would not serve as an accurate estimate of basin-scale pCO_2. Furthermore, our data showed little improvement in the relationship of pCO_2 with SST (R^2 = 0.537) over Landrum et al. (1996) and significantly supported Stephans et al. (1995) findings of poor predicting ability (RMSE = ±30.922 atm). Lee et al. (1998) also extrapolated surface pCO_2 in the Pacific Ocean based on the relationship of pCO_2 with SST and found low interannual variability in the recent CO_2 uptake of atmospheric pCO_2. Zhai et al. (2005) also reported underestimating field measurements of 0-50 µatm by the pCO_2-SST relationship in the Northern South China Sea. From the present results and literature, it is inferred that SST plays a vital role in the pCO_2 distribution and has a significant impact on the pCO_2 distribution in the Bay of Bengal.

IV. CONCLUSION

The seasonal regression analysis showed significant seasonal variability in the relationship of pCO_2 with SST. The pCO_2 and SST had a strong inverse relationship in all the seasons, suggesting that increased SST reduces CO_2 dissolution in seawater, lowering the pCO_2 in seawater. The distribution of pCO_2 fits well with the cubic curve in each season, and the best fit is found for the postmonsoon season. Further, an SST-based algorithm has been employed to generate *a* pCO_2 map using MODIS-Aqua-derived SST data. The validation of *the* pCO_2 map exhibited poor prediction capacity with an RMSE of ±30.922µatm. The satellite-derived pCO_2 map error is mainly because of the inbound errors in MODIS-derived SST products. As a result, advancements in sensor technology and retrieval algorithms will undoubtedly improve the retrieval of input parameters (SST), which will be valuable in accurately determining pCO_2. This would enable us to understand the biogeochemical processes behind the variability of CO_2 in the surface waters of the southwest Bay of Bengal.

ACKNOWLEDGMENTS

The authors are thankful to the Director, Dean, and the authorities of Annamalai University for their support and encouragement. The authors also thank the National Remote Sensing Centre, ISRO, Government of India, Hyderabad, for financial assistance through the NCP-Coastal Carbon Dynamics Study. The contents and views reported in the manuscript are of the individual authors and do not express the position or view of the organizations they present.

REFERENCES

[1] Barton, I. and A. Pearce: Validation of GLI and Other Satellite-Derived Sea Surface Temperatures Using Data from the Rottnest Island Ferry, Western Australia. Journal of Oceanography, 62 (2006) 303-310.

[2] Copin-Mont'egut, C.: A new formula for the effect of temperature on the partial pressure of CO_2 in seawater.Corrigendum. Marine Chemistry, 27 (1989) 143-144.

[3] Feely R. A., C. L. Sabine, T. Takahashi, and R. Wanninkhof: Uptake and storage of carbon dioxide in the Ocean: The Global CO_2 survey. Oceanography, 14(4) (2001) 18-32.

[4] Frankignoulle, M. and A.V. Borges: European continental shelf as a significant sink for atmospheric CO_2. Global Biogeochemical Cycles, 15(3) (2001) 569-576.

[5] Garbe, C.S., A. Rutgersson, J. Boutin, G. de Leeuw, B. Delille, C.W. Fairall, N. Gruber, J. Hare, D.T. Ho, M.T. Johnson, P.D. Nightingale, H. Pettersson, J. Piskozub, E. Sahlee W. Tsai, B. Ward, D.K. Woolf and C.J. Zappa: Transfer across the air-sea interface. In: Ocean-Atmosphere Interactions of Gases and Particles (Eds.: P.S. Liss and M.T. Johnson). Springer-Earth Sys. Sciences, Berlin, Heidelberg, (2014) 55-111.

[6] Gentemann, C.L.: Three-way validation of MODIS and AMSR-E sea surface temperatures. Journal of Geophysical Research: Oceans, 119 (2014) 2583-2598.

[7] Hosoda, K., H. Murakami, F. Sakaida and H. Kawamura: Algorithm and Validation of Sea Surface Temperature Observation Using MODIS Sensors Abroad Terra and Aqua in the Western North Pacific. Journal of Oceanography, 63 (2007) 267-280.

[8] IPCC: Carbon and other biogeochemical cycles. In: The Physical Science Basis. Contribution of Working Group I to the Fifth Assessment Report of the Intergovernmental Panel on Climate Change (Eds.: T. F. Stocker, D. Qun, G.K. Plattner, W. Tignor, S.K. Allen, J. Boschung, A. Nauels, Y. Xia, V. Bex, P.M. Midgley). Cambridge Univ. Press, Cambridge, (2013) 470-516.

[9] Keeling, R.F. and S. R. Shertz: Seasonal and interannual variations in atmospheric oxygen and implications for the global carbon cycle. Nat., 358 (1992) 723–727.

[10] Landrum, L.L., R.H. Gammon, R.A. Feely, P.P. Murphy, K.C. Kelly, C.E. Cosca and R. F. Weiss: North Pacific Ocean CO_2 disequilibrium for spring through summer, 1985–1989. Journal of Geophysical Research, 101(28) (1996) 539-555.

[11] Lee, K., R. Wanninkhof, T. Takahashi, S.C. Doney, and RA Feely: Low interannual variability in recent oceanic uptake of atmospheric carbon dioxide. Nature, 396 (1998) 155-159.

[12] Lee, T., S. Hakkinen, K. Kelly, B. Qiu, H. Bonekamp and E.J. Lindstrom: Satellite observations of ocean circulation changes with climate variability. Oceanography, 23(4) (2010) 70-81.

[13] Lefèvre, N. and A. Taylor: Estimating pCO_2 from sea surface temperatures in the Atlantic gyres. Deep-Sea Research, 49 (2002) 539-554.

[14] Lohrenz, S. E., and W. J. Cai: Satellite ocean color assessment of air-sea fluxes of CO_2 in a river-dominated coastal margin. Geophysical Research Letters, 33 (2006) L01601.

[15] Lu, J., F.L. Qiao, X.H. Wang, Y.G. Wang, Y. Teng, and C.S. Xia: A numerical study of transport dynamics and seasonal variability of the Yellow River sediment in the Bohai and Yellow seas. Estuarine Coastal Shelf Science, 95 (2011) 39-51.

[16] Metzl, N., A. Poisson, F. Louanchi, C. Brunet, B. Schauer, B. Bres: Spatio-temporal distributions of air–sea fluxes of CO_2 in the Indian and Antarctic oceans. Tellus., 47B (1995) 56-69.

[17] Narayanan, M., DT Vasan, AK Bharadwaj, P. Thanabalan, and N. Dhileeban: Comparison and validation of sea surface temperature (SST) using MODIS and AVHRR sensor data. International Journal of Remote Sensing and Geoscience, 2(3) (2013)1-7.

[18] Olsen, A., K.M. Brown, M. Chierici, T. Johannessen and C. Neill: Sea surface CO_2 fugacity in the subpolar North Atlantic. Biogeoscience, 5 (2008) 535-547.

[19] Ono, T., T. Saino, N. Kurita, and K. Sasaki: Basin-scale extrapolation of shipboard pCO_2 data by satellite SST and Chl a. International Journal of Remote Sensing, 25(19) (2004) 803-815.

[20] Bhavya, P. S., Sanjeev Kumar, G.V.M. Gupta, K.V. Sudharma, V. Sudheesh, and K. R. Dhanya: Carbon isotopic composition of suspended particulate matter and dissolved inorganic carbon in the Cochin estuary during postmonsoon. Current Science, 110(8) (2016) 1539-1543.

[21] Qin, B.Y., Z. Tao, Z.W. Li, and X.F. Yang: Seasonal changes and controlling factors of sea surface pCO_2 in the Yellow Sea. IOP conference series: Earth and Environmental Science, 17 (2014) 012025.

[22] Sabine, C.L., R. Wanninkhof, R.M. Key, C. Goyet and F.J. Millero: Seasonal CO_2 fluxes in the tropical and subtropical Indian Ocean. Marine Chemistry, 72, (2000) 33-55.

[23] Sarma, VVSS, T. Saino, K. Sasaoka, Y. Nojiri, T. Ono, M. Ishii, H.Y. Inoue, and K. Matsumoto: Basin-scale pCO_2 distribution using satellite sea surface temperature, Chl a, and climatological salinity in the North Pacific in spring and summer. Global Biogeochemical Cycles, 20 (2006) GB3005.

[24] Shanthi, R., D. Poornima, S. Raja, G. Vijaya Bhaskara Sethubathi and T. Thangaradjou: Validation of OCM-2 sensor performance in retrieving chlorophyll and TSM along the southwest Bay of Bengal coast. Journal of Earth System Science, 122(2) (2013) 479-489.

[25] Siegenthaler, U. and J.L. Sarmiento: Atmospheric carbon dioxide and the ocean, Nature, 365 (1993)119–125.

[26] Stephens, M.P., G. Samuels, D.B. Olson, R.A. Fine, and T. Takahashi: Sea-air flux of CO_2 in the North Pacific using shipboard and satellite data. Journal of Geophysical Research, 100 (1995)13571– 13583.

[27] Tans, PP, I.Y. Fung, and T. Takahashi: Observational constraints on the global atmospheric CO_2 budget. Science, 247 (1990)1431–1438.

[28] Wallace, D.W.R.: Monitoring global ocean carbon inventories, Background Rep. 5, Ocean Observation System Development Panel, Arlington, Va. (1995).

[29] Williams, G.N., A.I. Dogliotti, P. Zaidman, M. Solis, M.A. Narvarte, R.C. Gonzalez, J.L. Estevez, and D.A. Gagliardini: Assessment of Remotely-Sensed Sea-Surface Temperature and Chlorophyll-a Concentration in San Matías Gulf (Patagonia, Argentina). Continental Shelf Reserach, 52 (2013)159-171.

[30] Zhai, WD, M.H. Dai, W.J. Cai, Y.C. Wang, and Z.H. Wang: High partial pressure of CO2 and its maintaining mechanism in a subtropical estuary. The Pearl River estuary, China. Marine Chemistry, 93 (2005) 21-32.

[31] Zhu, Y., S. Shag, W. Zhai and M. Dai: Satellite-derived surface water pCO_2 and air-sea CO_2 fluxes in the northern South China Sea in Summer. Progress in Natural Science, 19 (2009) 775-779.

[32] Zui, T. A. O., Q. I. N. Bangyong, L. I. Ziwei, and Y. Xiaofeng: Satellite observations of the Partial Pressure of carbon dioxide in the surface water of the Huanghai Sea and the Bohai Sea. Acta Oceanologica Sinica, 31(3) (2012) 67-73.